





Article

Q-Balls in the Pseudogap Phase of Superconducting $\text{HgBa}_2\text{CuO}_{4+y}$

Gaetano Campi ^{1,*}, Luisa Barba ², Nikolai D. Zhigadlo ³, Andrey A. Ivanov ⁴, Alexey P. Menushenkov ⁴
and Antonio Bianconi ^{1,5,*}¹ Institute of Crystallography, CNR, Via Salaria Km 29.300, Monterotondo, 00015 Roma, Italy² Institute of Crystallography, CNR, Sincrotrone Elettra, Strada Statale 14—Km163.5, Area Science Park, Basovizza, 34149 Trieste, Italy³ CrystMat Company, CH-8037 Zurich, Switzerland⁴ Department of Solid State Physics and Nanosystems, National Research Nuclear University MEPhI (Moscow Engineering Physics Institute), Moscow 115409, Russia⁵ Rome International Center for Materials Science Superstripes RICMASS, Via dei Sabelli 119A, 00185 Roma, Italy

* Correspondence: gaetano.campi@ic.cnr.it (G.C.); antonio.bianconi@ricmass.eu (A.B.)

Abstract: Fast and local probes, such as X-ray spectroscopy, X-ray diffraction (XRD), and X-ray microscopy, have provided direct evidence for nanoscale phase separation in high temperature perovskite superconductors composed of (i) free particles coexisting with (ii) Jahn Teller polarons (i.e., charges associated with local lattice distortions) not detected by slow experimental methods probing only delocalized states. Moreover, these experimental probes have shown the formation of a superstripes phase in the pseudogap regime below T^* in cuprates. Here, we focus on the anomalous temperature dependence of short range X-ray diffraction CDW reflection satellites with high momentum transfer, probing both charge and lattice fluctuations in superconducting $\text{HgBa}_2\text{CuO}_{4+y}$ (Hg1201) in the pseudogap regime below T^* and above T_c . We report compelling evidence of the anomalous anticorrelation of the coherence volume with the peak maximum amplitude of the CDW XRD satellite by cooling below T^* . This anomalous temperature trend of the short-range striped Jahn Teller polaronic CDW puddles is in agreement with predictions of the Q-ball theory of the quark gluon plasma extended to cuprates, providing compelling evidence for non topological soliton puddles of striped condensate of pairs in the pseudogap phase.

Keywords: high temperature superconductivity; synchrotron X-ray diffraction; charge density waves; Q-balls



Citation: Campi, G.; Barba, L.; Zhigadlo, N.D.; Ivanov, A.A.; Menushenkov, A.P.; Bianconi, A. Q-Balls in the Pseudogap Phase of Superconducting $\text{HgBa}_2\text{CuO}_{4+y}$. *Condens. Matter* **2023**, *8*, 15. <https://doi.org/10.3390/condmat8010015>

Academic Editor:

Amir-Abbas Haghighirad

Received: 15 December 2022

Revised: 9 January 2023

Accepted: 11 January 2023

Published: 28 January 2023



Copyright: © 2023 by the authors. Licensee MDPI, Basel, Switzerland. This article is an open access article distributed under the terms and conditions of the Creative Commons Attribution (CC BY) license (<https://creativecommons.org/licenses/by/4.0/>).

1. Introduction

Recently, it has been proposed that the physics of Euclidean Q-balls developed in the frame of the quark-gluon plasma inside a proton in the atomic nucleus could be extended to the physics of complexity in high-temperature superconductivity [1]. In cuprates, short-range charge density waves (CDW) forming a supersolid phase called superstripes [2–4] have been observed by joint experiments of temperature-dependent X-ray diffraction (XRD) and scanning micro-XRD [2]. The superstripes phase [3,4] was also unveiled by X-ray absorption spectroscopy and anomalous diffraction experiments probing the condensation of polaronic charge density waves in striped puddles. Polarons involving localized charges with associated local lattice distortions, proposed by Bednorz and Müller [5], have been confirmed by experiments probing short-range order [6]. The X-ray absorption fine structure (EXAFS) [7,8] in X-ray spectroscopy, probing fast and local bond fluctuations, has been applied to cuprate superconductors, providing information on the polaron anisotropy, shown to be of pseudo-Jahn-Teller type, and on the large polaron size extending over eight copper sites [9–11]. The isotope effect [12] has been observed also at the pseudogap

temperature [13,14] associated with the onset of polaron ordering using X-ray absorption near edge structure (XANES) [15] a fast and local probe of many local body electronic configurations [16] and higher order atomic correlations in a nanoscale atomic cluster around Cu ions [17]. Pseudo-Jahn Teller polarons in cuprates have been confirmed by Goodenough et al. using thermopower experiments [18–22] probing electron-lattice vibronic coupling and heterogeneous charge fluctuations, forming a complex nanoscale phase separation as in colossal magneto-resistance manganite perovskites [23]. Nanoscale phase separation was predicted theoretically [24], and it has been the topic of two important workshops [25,26]. The complex landscape with the coexistence of two electronic components (free and localized charges) was confirmed by several experiments [27]. The experiments pointed toward the coexistence of undistorted stripes of charges in a strongly correlated doped charge-transfer Mott insulator with distorted stripes of polaronic charges. These experimental results provided the basis for the proposal of Bianconi-Perali-Valletta (BPV) theory in 1997 of multigap superconductivity in a striped nanoscale ultrastructure composed of a superlattice of quantum stripes. Here, the multigap superconductivity is generated by quantum size effects forming quantum minibands. The T_c amplification is driven by a Fano resonance due to configuration interaction between the first open pairing scattering channel forming BCS Cooper pairs composed of free particles in the first miniband and a second closed scattering channel forming pairs in the crossover of the *Bose-Einstein* Condensation (BEC) and *Bardeen-Cooper-Schrieffer* (BCS) (called the BEC-BCS crossover) with the formation of bipolarons in the intermediate coupling regime associated with strong electron-lattice interaction in the upper miniband. The coexistence of a first BCS condensate in the first miniband and a second BCS-BEC crossover condensate in the second miniband appears at a topological Lifshitz transition [28]. The discovery of high temperature superconductivity in layered multigap MgB_2 [29] confirmed the theoretical prediction of the amplification of the critical temperature also for a superlattice of quantum wells.

In this complex landscape, the essential ingredient in the mechanism of high-temperature superconductivity is the coexistence of two electronic components: (i) delocalized and weakly interacting itinerant particles, which coexist with (ii) localized and strongly interacting polarons. In perovskite materials, the polarons are formed by doped holes with the associated cloud of phonons and the formation of pairs of polarons. Using extended X-ray absorption fine structure (EXAFS) and X-ray absorption near edge structure (XANES), the probability distribution function of the instantaneous Cu-O bond length of the local lattice geometry has been determined, showing large nanoscale anisotropic pseudo-Jahn-Teller polarons forming instantaneous polaronic short-range CDW, which coexists with a Fermi liquid.

The formation of striped puddles of ordered polarons is driven by elastic attractive polaron-polaron interaction, which is zero when the polarons are in contact and it increases with the polaron-polaron distance. This attractive polaron-polaron force in hole-doped cuprate superconductors is analogous to the strong nuclear force between quarks forming the Q-balls, which competes with the repulsive Coulomb force between charges and determines the charge and the size of the short-range polaronic CDW puddle [30–33].

Using thermoelectric power experiments and thermal conductivity, Goodenough et al. have supported these results by showing vibronic strong electron-phonon coupling with a nonadiabatic regime, large low-symmetry polarons, and the formation of a striped lattice pattern, and they pointed out the similarity of nanoscale phase separation in manganites and cuprates with a striped texture [34–36].

Experiments of Müller, Shengelaya, Keller, Conradson, Mustre de Leon et al., and theory work of Bussmann-Holder, de Gennes, Deutscher, Bishop, Gorkov, Teitelbaum, and Kresin et al. have provided further evidence for the key role of local lattice fluctuations, complexity and charge and lattice heterogeneity in high-temperature superconductors [37–52]. In this paradigm, supported by a large set of different experimental methods and many different authors, the origin of the pseudogap phase below T^* and above T_c was assigned to the polaron coherence in high temperature superconducting cuprates with the formation of

isolated condensed nanoscale puddles of local pairs called superstripes [3,4]. EXAFS experiments have unveiled the double-well potential for oxygen vibration in the superconducting perovskite $\text{Ba}_{1-x}\text{K}_x\text{BiO}_3$ with the formation of a Fermi-Bose mixture with stripe-like nanoscale structural phase separation in superconducting in $\text{BaPb}_{1-x}\text{Bi}_x\text{O}_3$ [53–55]. Strong electron-lattice interaction, in particular hot spots in the k-space has been observed also in pressurized sulfur hydrides [56]. This confirms the universal scenario of two-component superconductivity in systems with strong unconventional electron-lattice interaction and ubiquitous unconventional short-range structural fluctuations and percolation, as has been confirmed recently in cuprates [57,58]. Recently, static CDW, long-range CDW, short-range CDW, and dynamic charge fluctuations have been observed by resonant X-ray scattering in cuprates pervading the full phase diagram [59–71] of cuprates and nickelates [72].

The proposed Euclidean Q-ball phase [1] may explain the pseudogap (PG) phase of high- T_c superconductivity in hole-doped high- T_c cuprates that precedes the multigap high- T_c superconducting phase with one particular large gap due to polaronic pairing in a strong coupling regime. This theory is based on a new physical mechanism for binding the fermions into local pairs via exchange with semiclassical density fluctuations of finite amplitude inside the Q-balls. The charge fluctuations inside the Q-balls possess a local minimum of potential energy at finite amplitude and, therefore, provide greater binding energy of fermions into local pairs than usually considered and also exchange infinitesimal spin-waves, charge-density fluctuations, or polaronic charge density waves (CDWs) in the Fröhlich picture. At couplings stronger than some critical values, local pairs percolate between Q-balls, forming a large superconducting cluster. We have used temperature-dependent X-ray diffraction (XRD) to test the theoretical predictions of the Q-ball temperature evolution [1]. We have selected a putative Q-ball reflection at a high momentum transfer [73,74], characterized by the reflection peak amplitude A being much higher than that of static weak CDW, with coherence volume V_{coh} smaller than that of static weak CDW appearing at a small momentum transfer, and the temperature onset at T^* being much higher than that of static CDW T_{CDW} , showing an anomalous temperature dependence of both the reflection peak amplitude A and V_{coh} . The measured temperature variation in the pseudogap phase has been found to agree with the prediction of the Q-ball theory [1], allowing us to attribute the nature of the selected short-range CDW to the presence of Q-balls in the pseudogap phase.

2. Results and Discussion

In this work, we focus on the puddles of short-range dynamical charge density fluctuations in the pseudogap phase in a high temperature superconductor, oxygen-doped $\text{HgBa}_2\text{CuO}_{4+y}$ (Hg1201). Hg1201 has a simple tetragonal average structure [75–87] with an optimum Cu-O bond length of 194 pm. It shows the self organization of dopants composed of atomic stripes of mobile oxygen interstitials (O-i) [81,82] running in both the horizontal (100) and vertical (010) directions in the ab plane. The nanoscale phase separation is composed of first puddles rich in O-i stripes that are anticorrelated with second puddles showing short-range dynamic charge density waves (CDW), which have been visualized by scanning micro-X-ray diffraction [2]. The $\text{HgBa}_2\text{CuO}_{4+y}$ single crystals have been grown [76] with a final oxygen treatment to establish a y concentration of oxygen interstitials of approximately $y = 0.12$, showing the superconducting optimum critical temperature T_c of 94 K [75–78]. The crystal structure has been determined by standard X-ray diffraction. The crystal structure has $P4/mmm$ symmetry with lattice parameters $a = b = 0.3886$ (5) nm and $c = 0.9517$ (2) nm at $T = 100$ K (numbers in parentheses indicate the standard deviation of the last digit, in agreement with reference [79]).

Short-range dynamic CDW puddles have been investigated by X-ray diffraction measurements performed at the XRD1 beamline of the ELETTRA synchrotron facility in Trieste, Italy. The charge modulation gives rise to clear superlattice reflections [1]. We have identified a particular satellite of a main Bragg diffraction peak assigned to a short-range dynamic CDW order in Hg1201, tuning the photon energy at 17.6 keV with a beam size

of $200 \times 200 \mu\text{m}^2$. The selected short-range dynamic CDW is located in the k-space at $q_{\text{CDW}} = (0.23, 0, 0.16)$ around the $(1, 0, 18)$ Bragg reflection.

We used a liquid nitrogen cryostat whose flux on the sample provided a variable temperature measured with an uncertainty of 1K. The cooling ramp was set with a step of 1K and a thermal waiting time of 10 min between two successive measurements. In order to reduce the temperature uncertainty, we averaged the collected data for every three measurements. The error bar at each temperature corresponds to the standard deviation of each group of three measurements.

To get a direct view of the temperature dependence of the short-range CDW-satellite reflection in the temperature range $85 < T < 280$ K, we show in Figure 1 the two-dimensional color plots of the CDW-peak profile along the a^* (top panel) and c^* (bottom panel) reciprocal lattice directions as a function of temperature. The selected peak appears as the sample was cooled below 240 K, which is close to the onset of the pseudogap phase T^* .

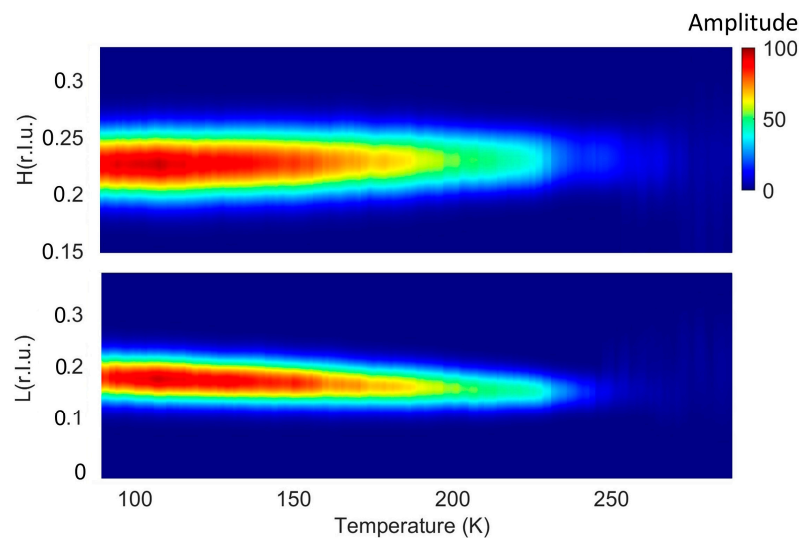


Figure 1. Color plots of temperature evolution of short-range CDW or charge fluctuations XRD profiles along (upper panel) a^* and (lower panel) c^* directions of reciprocal lattice around the $(1, 0, 18)$ Bragg peak.

The CDW-peak amplitude A at wavevectors $q_{\text{CDW}}(a^*)$, $q_{\text{CDW}}(c^*)$, and full widths at half maximum, $\Delta q_{\text{CDW}}(a^*)$, and $\Delta q_{\text{CDW}}(c^*)$, along both the in-plane a^* (H) and out-of-plane c^* (L) directions, have been extracted by fitting the CDW profiles with a Gaussian function after background subtraction. The coherence lengths ξ_a and ξ_c have been calculated as $\xi_a = a/\Delta q_{\text{CDW}}(a^*)$ and $\xi_c = b/\Delta q_{\text{CDW}}(c^*)$, where a and c are the crystallographic axes. The short-range dynamic CDW satellite shown in Figure 1 is assumed to be a putative Q-ball, which appears at the pseudogap temperature T^* . This temperature is higher than the temperature onset, $T_{\text{cdw}} = 159$ K, of the long-range static CDW weak reflections. In fact, static long-range CDW satellites are observed by resonant $\text{Cu } L_3$ X-ray scattering at small momentum transfer near the $l = 1$ main reflection in the approximate range from 0.26 to 0.29 r.l.u. [87]. Therefore, the selected satellite reflection is assigned to a short-range dynamical CDW detected in ref. [69] which is assigned to Q-balls made of pseudo-Jahn Teller polarons [88,89].

The CDW peak amplitude A , indicating the population of CDW puddles, reaches a maximum at $T = 100$ K, and then undergoes a drop associated with the onset of superconductivity at $T = T_c$, as shown in the three panels of Figure 2. The in-plane puddle size given by the coherence length ξ_a (along the a -axis) and out-of-plane ξ_c (along the c -axis) of CDW puddles can be inspected in Figure 2a,b, respectively. We observed smaller CDW puddles

along the c-axis. In Figure 2c, we report the coherence volume of the CDW puddles as given by:

$$V_{\text{coh}} = \xi_a \cdot \xi_a \cdot \xi_c \tag{1}$$

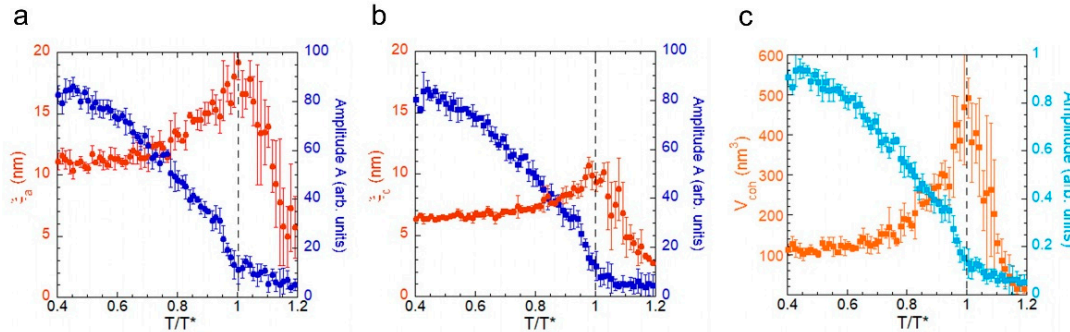


Figure 2. The short-range dynamic CDW-peak amplitude and coherence lengths as a function of the reduced temperature T/T^* (a) along the a-axis (ξ_a) and (b) along the c-axis (ξ_c). $T^* = 240$ K is the onset temperature for CDW in Hg1201. (c) Coherence volume, V_{coh} , with the amplitude peak as a function of reduced temperature. The vertical dashed lines indicate the onset of reduced temperature for CDW where $T = T^*$.

Recently, a new theory of the Euclidean Q-ball phase has been proposed [1]. It was demonstrated analytically that the Euclidean action of the strongly correlated electron system may possess stable saddle-point configurations in the form of finite-size puddles (Q-balls) with superconducting density fluctuations coupled to oscillating Matsubara-time fluctuations of charge or spin.

This Q-balls scenario is reminiscent of the famous Q-balls formation in the super-symmetric standard model, where the Noether charge responsible for the baryon number conservation is associated with the U(1) symmetry of the quarks’ field [1]. In condensed matter, the Q-Balls can be associated with the short-range charge density wave puddle; thus, we call Q-ball charge according to the Q-ball theory [1,90] as:

$$\text{Q-Ball} = T \cdot A \cdot V_{\text{coh}} \tag{2}$$

where T is the temperature, A is the CDW peak amplitude, and V_{coh} represents the coherence volume, given by Equation (1).

In Figure 3a, we show the behavior of the coherence volume V_{coh} as a function of the amplitude normalized to its maximum value. This behavior is well described by a power law $V_{\text{coh}} = C (A/A_{\text{max}})^{-\beta}$ where C is a constant and β is the critical exponent equal to 1.0 as predicted by the theory [90]. In Figure 3b,c, we report the temperature evolution of the product AV_{coh} and the temperute-dependent Q-Ball, respectively. The comparison of the Q-Ball temperature-dependent charge given by $T V_{\text{coh}} A$ measured in this experiment (black dots) with the theoretical curve calculated by Mukhin [90] (red curve) shows a very good agreement below $T^* = 240$ K, which is the critical temperature for the evaporation of the Q-ball.

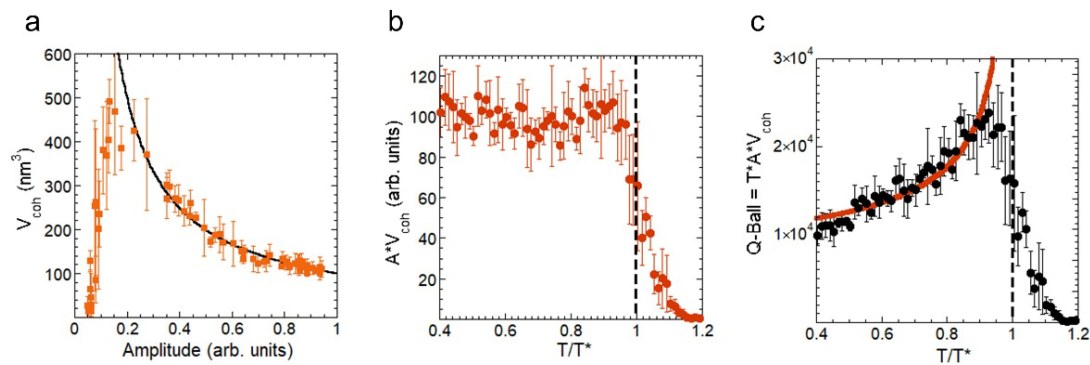


Figure 3. (a) Coherence volume, V_{coh} , as a function of the normalized CDW peak amplitude, A/A_{max} . The black line represents the fitting curve following the power-law $V_{\text{coh}} = C (A/A_{\text{max}})^{-1}$. (b) Coherence volume, V_{coh} , multiplied by CDW amplitude, A , and (c) Q-Ball = $T V_{\text{coh}} A$, as a function of the reduced temperature T/T^* , where $T^* = 240$ K. The red line represents the theoretical modeling elaborated by Mukhin [90].

3. Conclusions

We have used synchrotron radiation and X-ray diffraction to measure the short-range dynamic charge density waves (CDW) puddles in the optimum-doped $\text{HgBa}_2\text{CuO}_{4+y}$ with $y = 0.12$ and $T_c = 94$ K. We have found a short-range incommensurate CDW reflection with wavevector $q_{\text{CDW}} = (0.23, 0, 0.16)$ around the Bragg peak $(1, 0, 18)$ below $T^* = 240$ K, which is assigned to a dynamic short-range CDW. We have extracted the CDW peak amplitude, wavevector, and coherence length as a function of the temperature from room temperature down to 85 K. The experimental results on the temperature evolution of the dynamic short-range CDW puddles in the superconducting $\text{HgBa}_2\text{CuO}_{4+y}$ may be interpreted in terms of the Euclidean Q-Balls theory [1,90]. Finally, after decades of experimental and theoretical research on high-temperature copper perovskites, the complexity of these systems is due to a nanoscale phase separation composed of coexisting (i) atomic wires of oxygen interstitials with a scale-free distribution, (ii) static long-range CDW puddles, observed in resonant X-ray scattering at low momentum transfer [87], and (iii) dynamic short-range Q-balls, which have been called charge density fluctuations [69], which show similarity with the case of doped $\text{La}_{2-x}\text{Sr}_x\text{NiO}_4$ where dynamic short-range CDW coexist with quasi-static long-range CDW in different spatial locations [72]. Further and more extensive experimental work investigating the spatial distribution and time evolution of the short-range polaronic CDW puddles is in progress to enforce the proposed analogy between the Q-ball scenario and short-range CDW puddles appearing at the pseudogap temperature, T^* , in cuprates.

Author Contributions: Conceptualization, G.C. and A.B.; methodology, A.B., L.B., G.C., A.A.I. and A.P.M.; software, G.C.; validation, G.C. and A.B.; crystal growth, N.D.Z.; data curation, G.C., A.B., L.B., A.A.I. and A.P.M.; writing—original draft preparation, A.B., G.C., A.A.I. and A.P.M.; writing—review and editing, G.C., A.B. and A.A.I.; funding acquisition, A.B., A.A.I. and A.P.M. All authors have read and agreed to the published version of the manuscript.

Funding: This research received funding from Superstripes onlus.

Institutional Review Board Statement: Not applicable.

Informed Consent Statement: Not applicable.

Data Availability Statement: The data that support the findings of this study are available from the corresponding author, (G.C.), upon reasonable request.

Acknowledgments: We thank Sergei Mukhin for the discussions and for sharing his theoretical results before publication. We are grateful to the Elettra beamline staff for their experimental help. A.A.I. and A.P.M. acknowledge the support of the Ministry of Science and Higher Education of the Russian Federation (Agreement no. 075-15-2021-1352).

Conflicts of Interest: The authors declare no conflict of interest. The funders had no role in the design of the study; in the collection, analyses, or interpretation of data; in the writing of the manuscript; or in the decision to publish the results.

References

1. Mukhin, S. Euclidean Q-balls of fluctuating sdw/cdw in the ‘nested’ hubbard model of high- T_c superconductors as the origin of pseudogap and superconducting behaviors. *Condens. Matter* **2022**, *7*, 31. [[CrossRef](#)]
2. Campi, G.; Bianconi, A.; Poccia, N.; Barba, L.; Arrighetti, G.; Innocenti, D.; Karpinski, J.; Zhigadlo, N.D.; Kazakov, S.M.; Burghammer, M.; et al. Inhomogeneity of charge-density-wave order and quenched disorder in a high- T_c superconductor. *Nature* **2015**, *525*, 359–362. [[CrossRef](#)] [[PubMed](#)]
3. Bianconi, A. Superstripes. *Int. J. Mod. Phys. B* **2000**, *14*, 3289–3297. [[CrossRef](#)]
4. Bianconi, A. Shape resonances in superstripes. *Nat. Phys.* **2013**, *9*, 536–537. [[CrossRef](#)]
5. Bednorz, J.G.; Müller, K.A. Perovskite-type oxides—The new approach to high- T_c superconductivity. *Rev. Mod. Phys.* **1988**, *60*, 585. [[CrossRef](#)]
6. Egami, T. Alex and the origin of high-temperature superconductivity. In *High- T_c Copper Oxide Superconductors and Related Novel Materials*; Springer: Cham, Switzerland, 2017; pp. 35–46.
7. Kronig, R.D.L. Zur theorie der feinstruktur in den röntgenabsorptionsspektren. *Z. Phys.* **1931**, *70*, 317–323. [[CrossRef](#)]
8. Kronig, R.D.L. Zur theorie der feinstruktur in den Röntgenabsorptionsspektren. II. *Z. Phys.* **1932**, *75*, 191–210. [[CrossRef](#)]
9. Bianconi, A. On the Fermi liquid coupled with a generalized Wigner polaronic CDW giving high T_c superconductivity. *Solid State Commun.* **1994**, *91*, 1–5. [[CrossRef](#)]
10. Bianconi, A.; Missori, M.; Oyanagi, H.; Yamaguchi, H.; Ha, D.H.; Nishiara, Y.; Della Longa, S. The measurement of the polaron size in the metallic phase of cuprate superconductors. *EPL Europhys. Lett.* **1995**, *31*, 411. [[CrossRef](#)]
11. Bianconi, A.; Saini, N.L.; Lanzara, A.; Missori, M.; Rossetti, T.; Oyanagi, H.; Yamaguchi, H.; Oka, K.; Ito, T. Determination of the local lattice distortions in the CuO₂ plane of La_{1.85}Sr_{0.15}CuO₄. *Phys. Rev. Lett.* **1996**, *76*, 3412. [[CrossRef](#)]
12. Zhao, G.M.; Conder, K.; Keller, H.; Müller, K.A. Oxygen isotope effects in: Evidence for polaronic charge carriers and their condensation. *J. Phys. Condens. Matter* **1998**, *10*, 9055. [[CrossRef](#)]
13. Lanzara, A.; Zhao, G.M.; Saini, N.L.; Bianconi, A.; Conder, K.; Keller, H.; Müller, K.A. Oxygen-isotope shift of the charge-stripe ordering temperature in La_{2-x}Sr_xCuO₄ from x-ray absorption spectroscopy. *J. Phys. Condens. Matter* **1999**, *11*, L541. [[CrossRef](#)]
14. Bendele, M.; Von Rohr, F.; Guguchia, Z.; Pomjakushina, E.; Conder, K.; Bianconi, A.; Simon, A.; Bussman-Holder, A.; Keller, H. Evidence for strong lattice effects as revealed from huge unconventional oxygen isotope effects on the pseudogap temperature in La_{2-x}Sr_xCuO₄. *Phys. Rev. B* **2017**, *95*, 014514. [[CrossRef](#)]
15. Della Longa, S.; Soldatov, A.; Pompa, M.; Bianconi, A. Atomic and electronic structure probed by X-ray absorption spectroscopy: Full multiple scattering analysis with the G4XANES package. *Comput. Mater. Sci.* **1995**, *4*, 199–210. [[CrossRef](#)]
16. Bianconi, A.; Bauer, R.S. Evidence of SiO at the Si-oxide interface by surface soft X-ray absorption near edge spectroscopy. *Surf. Sci.* **1980**, *99*, 76–86. [[CrossRef](#)]
17. Bianconi, A. Multiplet splitting of final-state configurations in x-ray-absorption spectrum of metal VO₂: Effect of core-hole-screening, electron correlation, and metal-insulator transition. *Phys. Rev. B* **1982**, *26*, 2741. [[CrossRef](#)]
18. Goodenough, J.B.; Zhou, J.S.; Bersuker, G.I. Thermoelectric Power and normal state of the high- T_c copper oxides. In Proceedings of the International Workshop on Anharmonic-Properties of High- T_c cuprates, Bled, Slovenia, 1–6 September 1994.
19. Zhou, J.S.; Bersuker, G.I.; Goodenough, J.B. Non-adiabatic electron-lattice interactions in the copper-oxide superconductors. *J. Supercond.* **1995**, *8*, 541–544. [[CrossRef](#)]
20. Bersuker, G.I.; Goodenough, J.B. Large low-symmetry polarons of the high- T_c copper oxides: Formation, mobility and ordering. *Phys. C Supercond.* **1997**, *274*, 267–285. [[CrossRef](#)]
21. Goodenough, J.B.; Zhou, J.S. Vibronic states in La_{2-x}Ba_xCuO₄. *J. Supercond.* **1997**, *10*, 309–314. [[CrossRef](#)]
22. Zhou, J.S.; Goodenough, J.B. Electron-lattice coupling and stripe formation in La_{2-x}Ba_xCuO₄. *Phys. Rev. B* **1997**, *56*, 6288. [[CrossRef](#)]
23. Goodenough, J.B.; Zhou, J.S. New forms of phase segregation. *Nature* **1997**, *386*, 229–230. [[CrossRef](#)]
24. Kremer, R.K.; Hizhnyakov, V.; Sigmund, E.; Simon, A.; Müller, K.A. Electronic phase separation in La-cuprates. *Z. Phys. B Condens. Matter* **1993**, *91*, 169–174. [[CrossRef](#)]
25. Müller, K.A.; Benedek, G. (Eds.) Phase Separation in cuprate superconductors. In Proceedings of the Workshop Phase Separation in Cuprate Superconductors Held in Erice, Erice, Italy, 6–9 May 1992; World Scientific: Singapore, 1993.
26. Sigmund, E.; Müller, K.A. (Eds.) Phase Separation in Cuprate Superconductors. In Proceedings of the Second International Workshop on “Phase Separation in Cuprate Superconductors”, Cottbus, Germany, 4–10 September 1993; Springer Science Business Media: Berlin/Heidelberg, Germany, 2012.
27. Müller, K.A.; Zhao, G.M.; Conder, K.; Keller, H. The ratio of small polarons to free carriers in derived from susceptibility measurements. *J. Phys. Condens. Matter* **1998**, *10*, L291. [[CrossRef](#)]
28. Bianconi, A.; Valletta, A.; Perali, A.; Saini, N.L. Superconductivity of a striped phase at the atomic limit. *Phys. C Supercond.* **1998**, *296*, 269–280. [[CrossRef](#)]

29. Bauer, E.; Paul, C.; Berger, S.; Majumdar, S.; Michor, H.; Giovannini, M.; Saccone, A.; Bianconi, A. Thermal conductivity of superconducting MgB₂. *J. Phys. Condens. Matter* **2001**, *13*, L487. [[CrossRef](#)]
30. Kusmartsev, F.V.; Di Castro, D.; Bianconi, G.; Bianconi, A. Transformation of strings into an inhomogeneous phase of stripes and itinerant carriers. *Phys. Lett. A* **2000**, *275*, 118–123. [[CrossRef](#)]
31. Kusmartsev, F.V. Electron strings in oxides. In *Phase Transitions and Self-Organization in Electronic and Molecular Networks*; Springer: Boston, MA, USA, 2002.
32. Kusmartsev, F.V.; Saarela, M. Dipolar clusters and ferroelectricity in high T_c superconductors. *Int. J. Mod. Phys. B* **2015**, *29*, 1542002. [[CrossRef](#)]
33. Saarela, M.; Kusmartsev, F.V. Phase transitions to dipolar clusters and charge density waves in high T_c superconductors. *Phys. C Supercond. Appl.* **2017**, *533*, 9–19. [[CrossRef](#)]
34. Goodenough, J.B.; Zhou, J.S. Enhanced thermoelectric power and stripes in cuprate superconductors. In *Stripes and Related Phenomena*; Springer: Boston, MA, USA, 2002; pp. 199–209.
35. Yan, J.Q.; Zhou, J.S.; Goodenough, J.B. Thermal conductivity in the stripe-ordered phase of cuprates and nickelates. *Phys. Rev. B* **2003**, *68*, 104520. [[CrossRef](#)]
36. Goodenough, J.B. Ordering of bond length fluctuations in the copper-oxide superconductors. *EPL Europhys. Lett.* **2002**, *57*, 550. [[CrossRef](#)]
37. Shengelaya, A.; Bruun, M.; Kochelaev, B.I.; Safina, A.; Conder, K.; Müller, K.A. Microscopic Phase Separation and two type of quasiparticles in lightly doped La_{2-x}Sr_xCuO₄ observed by electron paramagnetic resonance. In *Symmetry and Heterogeneity in High Temperature Superconductors*; Springer: Dordrecht, The Netherlands, 2006; pp. 105–116.
38. Müller, K.A. Electron paramagnetic resonance and high temperature superconductivity. *J. Supercond. Nov. Magn.* **2006**, *19*, 53–57. [[CrossRef](#)]
39. Campi, G.; Cappelluti, E.; Proffen, T.; Qiu, X.; Bozin, E.S.; Billinge, S.J.L.; Agrestini, S.; Saini, N.L.; Bianconi, A. Study of temperature dependent atomic correlations in MgB₂. *Eur. Phys. J. B-Condens. Matter Complex Syst.* **2006**, *52*, 15–21. [[CrossRef](#)]
40. Shengelaya, A.; Müller, K.A. The intrinsic heterogeneity of superconductivity in the cuprates. *EPL Europhys. Lett.* **2015**, *109*, 27001. [[CrossRef](#)]
41. Müller, K.A. Essential heterogeneities in hole-doped cuprate superconductors. In *Intrinsic Multiscale Structure and Dynamics in Complex Electronic Oxides*; World Scientific: Singapore, 2003; pp. 1–5.
42. Müller, K.A.; Bussmann-Holder, A. (Eds.) *Superconductivity in Complex Systems*; Springer: Berlin/Heidelberg, Germany, 2005; Volume 114.
43. Deutscher, G.; de Gennes, P.G. A spatial interpretation of emerging superconductivity in lightly doped cuprates. *Comptes Rendus Phys.* **2007**, *8*, 937–941. [[CrossRef](#)]
44. Keller, H.; Bussmann-Holder, A.; Müller, K.A. Jahn–Teller physics and high-T_c superconductivity. *Mater. Today* **2008**, *11*, 38–46. [[CrossRef](#)]
45. Müller, K.A. The unique properties of superconductivity in cuprates. *J. Supercond. Nov. Magn.* **2014**, *27*, 2163–2179. [[CrossRef](#)]
46. Müller, K.A. The polaronic basis for high-temperature superconductivity. *J. Supercond. Nov. Magn.* **2017**, *30*, 3007–3018. [[CrossRef](#)]
47. Bussmann-Holder, A.; Keller, H.; Bishop, A.R.; Simon, A.; Müller, K.A. Polaron coherence as origin of the pseudogap phase in high temperature superconducting cuprates. *J. Supercond. Nov. Magn.* **2008**, *21*, 353–357. [[CrossRef](#)]
48. Barišić, N.; Sunko, D.K. High-T_c cuprates: A story of two electronic subsystems. *J. Supercond. Nov. Magn.* **2022**, *35*, 1781–1799. [[CrossRef](#)]
49. Krockenberger, Y.; Ikeda, A.; Yamamoto, H. Atomic stripe formation in infinite-layer cuprates. *ACS Omega* **2021**, *6*, 21884–21891. [[CrossRef](#)]
50. Conradson, S.D.; Geballe, T.H.; Gauzzi, A.; Karppinen, M.; Jin, C.; Baldinozzi, G.; Li, W.; Cao, L.; Gilioli, E.; Jiang, J.M.; et al. Local lattice distortions and dynamics in extremely overdoped superconducting YSr₂Cu_{2.75}Mo_{0.25}O_{7.54}. *Proc. Natl. Acad. Sci. USA* **2020**, *117*, 4559–4564. [[CrossRef](#)] [[PubMed](#)]
51. Velasco, V.; Neto, M.B.S.; Perali, A.; Wimberger, S.; Bishop, A.R.; Conradson, S.D. Kuramoto synchronization of quantum tunneling polarons for describing the dynamic structure in cuprate superconductors. *Phys. Rev. B* **2022**, *105*, 174305. [[CrossRef](#)]
52. Velasco, V.; Silva Neto, M.B.; Perali, A.; Wimberger, S.; Bishop, A.R.; Conradson, S.D. Evolution of Charge-Lattice Dynamics across the Kuramoto Synchronization Phase Diagram of Quantum Tunneling Polarons in Cuprate Superconductors. *Condens. Matter* **2021**, *6*, 52. [[CrossRef](#)]
53. Menushenkov, A.P.; Klementev, K.V. Extended x-ray absorption fine-structure indication of a double-well potential for oxygen vibration in Ba_{1-x}K_xBiO₃. *J. Phys. Condens. Matter* **2000**, *12*, 3767. [[CrossRef](#)]
54. Menushenkov, A.P.; Kuznetsov, A.V.; Klementiev, K.V.; Kagan, M.Y. Fermi-Bose mixture in Ba (K) BiO₃ superconducting oxide. *J. Supercond. Nov. Magn.* **2016**, *29*, 701–705. [[CrossRef](#)]
55. Giraldo-Gallo, P.; Zhang, Y.; Parra, C.; Manoharan, H.C.; Beasley, M.R.; Geballe, T.H.; Kramer, M.J.; Fisher, I.R. Stripe-like nanoscale structural phase separation in superconducting BaPb_{1-x}Bi_xO₃. *Nat. Commun.* **2015**, *6*, 8231. [[CrossRef](#)]
56. Bianconi, A.; Jarlborg, T. Lifshitz transitions and zero point lattice fluctuations in sulfur hydride showing near room temperature superconductivity. *Nov. Supercond. Mater.* **2015**, *1*, 37–49. [[CrossRef](#)]
57. Popčević, P.; Pelc, D.; Tang, Y.; Velebit, K.; Anderson, Z.; Nagarajan, V.; Yu, G.; Požek, M.; Barišić, N.; Greven, M. Percolative nature of the direct-current paraconductivity in cuprate superconductors. *NPJ Quantum Mater.* **2018**, *3*, 42. [[CrossRef](#)]

58. Pelc, D.; Spieker, R.J.; Anderson, Z.W.; Krogstad, M.J.; Biniskos, N.; Bielinski, N.G.; Yu, B.; Sasagawa, T.; Chauviere, L.; Dosanjh, P.; et al. Unconventional short-range structural fluctuations in cuprate superconductors. *Sci. Rep.* **2022**, *12*, 20483. [[CrossRef](#)]
59. Caprara, S.; Di Castro, C.; Seibold, G.; Grilli, M. Dynamical charge density waves rule the phase diagram of cuprates. *Phys. Rev. B* **2017**, *95*, 224511. [[CrossRef](#)]
60. Arpaia, R.; Caprara, S.; Fumagalli, R.; De Vecchi, G.; Peng, Y.Y.; Andersson, E.; Betto, D.; De Luca, G.M.; Brookes, N.B.; Lombardi, F.; et al. Dynamical charge density fluctuations pervading the phase diagram of a Cu-based high- T_c superconductor. *Science* **2019**, *365*, 906–910. [[CrossRef](#)] [[PubMed](#)]
61. Wen, J.J.; Huang, H.; Lee, S.J.; Jang, H.; Knight, J.; Lee, Y.S.; Fujita, M.; Suzuki, K.M.; Asano, S.; Kivelson, S.A.; et al. Observation of two types of charge-density-wave orders in superconducting $\text{La}_{2-x}\text{Sr}_x\text{CuO}_4$. *Nat. Commun.* **2019**, *10*, 3269. [[CrossRef](#)] [[PubMed](#)]
62. Miao, H.; Fumagalli, R.; Rossi, M.; Lorenzana, J.; Seibold, G.; Yakhou-Harris, F.; Kummer, K.; Brookes, N.B.; Gu, G.D.; Braicovich, L.; et al. Formation of incommensurate charge density waves in cuprates. *Phys. Rev. X* **2019**, *9*, 031042. [[CrossRef](#)]
63. Cremin, K.A.; Zhang, J.; Homes, C.C.; Gu, G.D.; Sun, Z.; Fogler, M.M.; Millis, A.J.; Basov, D.N.; Averitt, R.D. Photoenhanced metastable c-axis electrostatics in stripe-ordered cuprate $\text{La}_{1.885}\text{Ba}_{0.115}\text{CuO}_4$. *Proc. Natl. Acad. Sci. USA* **2019**, *116*, 19875–19879. [[CrossRef](#)] [[PubMed](#)]
64. Yu, G.; Xia, D.D.; Pelc, D.; He, R.H.; Kaneko, N.H.; Sasagawa, T.; Li, Y.; Zhao, X.; Barišić, N.; Shekhter, A.; et al. Universal precursor of superconductivity in the cuprates. *Phys. Rev. B* **2019**, *99*, 214502. [[CrossRef](#)]
65. Pelc, D.; Popčević, P.; Požek, M.; Greven, M.; Barišić, N. Unusual behavior of cuprates explained by heterogeneous charge localization. *Sci. Adv.* **2019**, *5*, eaau4538. [[CrossRef](#)]
66. Caprara, S. The ancient romans' route to charge density waves in cuprates. *Condens. Matter* **2019**, *4*, 60. [[CrossRef](#)]
67. Lin, J.Q.; Miao, H.; Mazzone, D.G.; Gu, G.D.; Nag, A.; Walters, A.C.; García-Fernández, M.; Barbour, A.; Pellicciari, J.; Jarrige, I.; et al. Strongly correlated charge density wave in $\text{La}_{2-x}\text{Sr}_x\text{CuO}_4$ evidenced by doping-dependent phonon anomaly. *Phys. Rev. Lett.* **2020**, *124*, 207005. [[CrossRef](#)]
68. Chen, X.M.; Mazzoli, C.; Cao, Y.; Thampy, V.; Barbour, A.M.; Hu, W.; Lu, M.; Assefa, T.A.; Miao, H.; Fabbri, G.; et al. Charge density wave memory in a cuprate superconductor. *Nat. Commun.* **2019**, *10*, 1435. [[CrossRef](#)] [[PubMed](#)]
69. Yu, B.; Tabis, W.; Bialo, I.; Yakhou, F.; Brookes, B.; Anderson, Z.; Tang, Y.; Yu, G.; Greven, M. Unusual dynamic charge correlations in simple-tetragonal $\text{HgBa}_2\text{CuO}_{4+\delta}$. *Phys. Rev. X* **2020**, *10*, 021059. [[CrossRef](#)]
70. Seibold, G.; Arpaia, R.; Peng, Y.Y.; Fumagalli, R.; Braicovich, L.; Di Castro, C.; Grilli, M.; Ghiringhelli, G.C.; Caprara, S. Strange metal behaviour from charge density fluctuations in cuprates. *Commun. Phys.* **2021**, *4*, 7. [[CrossRef](#)]
71. Miao, H.; Fabbri, G.; Koch, R.J.; Mazzone, D.G.; Nelson, C.S.; Acevedo-Estevés, R.; Gu, G.D.; Li, Y.; Yilmaz, T.; Kaznatcheev, K.; et al. Charge density waves in cuprate superconductors beyond the critical doping. *NPJ Quantum Mater.* **2021**, *6*, 31. [[CrossRef](#)]
72. Campi, G.; Bianconi, A.; Joseph, B.; Mishra, S.K.; Muller, L.; Zozulya, A.; Nugroho, A.A.; Roy, S.; Sprung, M.; Ricci, A. Nanoscale inhomogeneity of charge density waves dynamics in $\text{La}_{2-x}\text{Sr}_x\text{NiO}_4$. *Sci. Rep.* **2022**, *12*, 15964. [[CrossRef](#)] [[PubMed](#)]
73. Croft, T.; Lester, C.J.; Senn, M.S.; Bombardi, A.; Hayden, S.M. Charge density wave fluctuations in $\text{La}_{2-x}\text{Sr}_x\text{CuO}_4$ and their competition with superconductivity. *Phys. Rev. B* **2014**, *89*, 224513. [[CrossRef](#)]
74. Forgan, E.; Blackburn, E.; Holmes, A.; Briffa, A.K.R.; Chang, J.; Bouchenoire, L.; Brown, S.D.; Liang, R.; Bonn, D.; Hardy, W.N.; et al. The microscopic structure of charge density waves in underdoped $\text{YBa}_2\text{Cu}_3\text{O}_{6.54}$ revealed by X-ray diffraction. *Nat. Commun.* **2015**, *6*, 10064. [[CrossRef](#)]
75. Putilin, S.; Antipov, E.; Chmaissem, O.; Marezio, M.J.N. Superconductivity at 94 K in $\text{HgBa}_2\text{CuO}_{4+\delta}$. *Nature* **1993**, *362*, 226–228. [[CrossRef](#)]
76. Karpinski, J.; Meijer, G.I.; Schwer, H.; Molinski, R.; Kopnin, E.; Conder, K.; Angst, M.; Jun, J.; Kazakov, S.; Wisniewski, A.; et al. High-pressure synthesis, crystal growth, phase diagrams, structural and magnetic properties of $\text{Y}_2\text{Ba}_4\text{Cu}_n\text{O}_{2n+x}$, $\text{HgBa}_2\text{Ca}_{n-1}\text{Cu}_n\text{O}_{2n+2+x}$ and quasi-one-dimensional cuprates. *Supercond. Sci. Technol.* **1999**, *12*, R153–R181. [[CrossRef](#)]
77. Legros, A.; Loret, B.; Forget, A.; Bonnaillie, P.; Collin, G.; Thuéry, P.; Sacuto, A.; Colson, D. Crystal growth and doping control of $\text{HgBa}_2\text{CuO}_{4+\delta}$, the model compound for high- T_c superconductors. *Mater. Res. Bull.* **2019**, *118*, 110479. [[CrossRef](#)]
78. Bordet, P.; Duc, F.; LeFloch, S.; Capponi, J.J.; Alexandre, E.; Rosa-Nunes, M.; Putilin, S.; Antipov, E.V. Single crystal X-ray diffraction study of the $\text{HgBa}_2\text{CuO}_{4+\delta}$ superconducting compound. *Phys. C Supercond.* **1996**, *271*, 189–196. [[CrossRef](#)]
79. Balagurov, A.M.; Sheptyakov, D.V.; Aksenov, V.L.; Antipov, E.V.; Putilin, S.N.; Radaelli, P.G.; Marezio, M. Structure of $\text{HgBa}_2\text{CuO}_{4+\delta}$ ($0.06 < \delta < 0.19$) at ambient and high pressure. *Phys. Rev. B* **1999**, *59*, 7209–7215. [[CrossRef](#)]
80. Auvray, N.; Loret, B.; Chibani, S.; Grasset, R.; Guarnelli, Y.; Parisiades, P.; Forget, A.; Colson, D.; Cazayous, M.; Gallais, Y.; et al. Exploration of Hg-based cuprate superconductors by Raman spectroscopy under hydrostatic pressure. *Phys. Rev. B* **2021**, *103*, 19513. [[CrossRef](#)]
81. Izquierdo, M.; Megtert, S.; Colson, D.; Honkimäki, V.; Forget, A.; Raffy, H.; Comès, R. One dimensional ordering of doping oxygen in superconductors evidenced by x-ray diffuse scattering. *J. Phys. Chem. Solids* **2011**, *72*, 545–548. [[CrossRef](#)]
82. Izquierdo, M.; Freitas, D.C.; Colson, D.; Garbarino, G.; Forget, A.; Raffy, H.; Itié, J.-P.; Ravy, S.; Fertey, P.; Núñez-Regueiro, M. Charge order and suppression of superconductivity in $\text{HgBa}_2\text{CuO}_{4+\delta}$ at high pressures. *Condens. Matter* **2021**, *6*, 25. [[CrossRef](#)]
83. Barbiellini, B.; Jarlborg, T. Electron and positron states in $\text{HgBa}_2\text{CuO}_4$. *Phys. Rev. B* **1994**, *50*, 3239. [[CrossRef](#)] [[PubMed](#)]
84. Ambrosch-Draxl, C.; Sherman, E.Y. Inhomogeneity effects in oxygen-doped $\text{HgBa}_2\text{CuO}_4$. *Phys. Rev. B* **2006**, *74*, 024503. [[CrossRef](#)]
85. Wang, S.; Zhang, J.; Yan, J.; Che, X.-J.; Struzhkin, V.; Tabis, W.; Barisic, N.; Chan, M.K.; Dorow, C.; Zhao, X.; et al. Strain derivatives of T_c in $\text{HgBa}_2\text{CuO}_{4+\delta}$: The CuO_2 plane alone is not enough. *Phys. Rev. B* **2014**, *89*, 024515. [[CrossRef](#)]

86. Ohgoe, T.; Hirayama, M.; Misawa, T.; Ido, K.; Yamaji, Y.; Imada, M. Ab initio study of superconductivity and inhomogeneity in a Hg-based cuprate superconductor. *Phys. Rev. B* **2020**, *101*, 045124. [[CrossRef](#)]
87. Tabis, W.; Yu, B.; Bialo, I.; Bluschke, M.; Kolodziej, T.; Kozłowski, A.; Blackburn, E.; Sen, K.; Forgan, E.M.; Zimmermann, M.; et al. Synchrotron x-ray scattering study of charge-density-wave order in $\text{HgBa}_2\text{CuO}_{4+\delta}$. *Phys. Rev. B* **2017**, *96*, 134510. [[CrossRef](#)]
88. Clougherty, D.P.; Foell, C.A. Vector polarons in a degenerate electron system. *Phys. Rev. B* **2004**, *70*, 052301. [[CrossRef](#)]
89. Clougherty, D.P. Jahn-Teller solitons, structural phase transitions, and phase separation. *Phys. Rev. Lett.* **2006**, *96*, 045703. [[CrossRef](#)]
90. Mukhin, S. Possible manifestation of Q-ball mechanism of high T_c superconductivity in X-ray diffraction. *Condens. Matter* **2022**, *8*, 16. [[CrossRef](#)]

Disclaimer/Publisher's Note: The statements, opinions and data contained in all publications are solely those of the individual author(s) and contributor(s) and not of MDPI and/or the editor(s). MDPI and/or the editor(s) disclaim responsibility for any injury to people or property resulting from any ideas, methods, instructions or products referred to in the content.